

Cancer-Associated Fibroblasts Promote Angiogenesis of Hepatocellular Carcinoma by VEGF-Mediated EZH2/VASH1 Pathway

Technology in Cancer Research & Treatment
Volume 18: 1-12
© The Author(s) 2019
Article reuse guidelines:
sagepub.com/journals-permissions
DOI: 10.1177/1533033819879905
journals.sagepub.com/home/tct


Bin Huang, MM¹, Manping Huang, MM¹, and Qin Li, BS² 

Abstract

Background: Hepatocellular carcinoma is a highly vascularized tumor, so it is critical to study its angiogenesis. Cancer-associated fibroblasts and enhancer of zeste homolog 2 play an important role in tumor angiogenesis and became significant hallmarks of cancer. But the relationship between enhancer of zeste homolog-2 and cancer-associated fibroblasts in response to angiogenesis and its precise mechanism remains unclear. **Methods:** The separation of cancer-associated fibroblasts was identified by immunofluorescence. 3-(4,5-Dimethylthiazol-2-yl)-2,5-diphenyltetrazolium bromide analysis was used to reveal the proliferation of human umbilical vein endothelial cells. Vascular endothelial growth factor level was quantified by enzyme-linked immunosorbent assay. The wound healing, transwell, and vascular tube formation assays were used to identify the capability of migration, invasion, and tube formation of human umbilical vein endothelial cells *in vitro*. The detection of tumor angiogenesis was also performed *in vivo*. Finally, the level of enhancer of zeste homolog-2 and vasohibin 1 were determined by quantitative real-time polymerase chain reaction and Western blotting. **Results:** In comparison to control and condition medium noncancerous fibroblasts groups, the condition medium cancer-associated fibroblasts could significantly promote the proliferation, migration, invasion, and angiogenesis of human umbilical vein endothelial cells. We found that cancer-associated fibroblasts promoted angiogenesis of human umbilical vein endothelial cells via vascular endothelial growth factor secretion *in vitro* and *in vivo*. The upregulation of enhancer of zeste homolog 2 by vascular endothelial growth factor inhibited the expression of vasohibin 1, thus promoting the proliferation and angiogenesis of human umbilical vein endothelial cells. Taken together, the cancer-associated fibroblasts of hepatocellular carcinoma regulate the enhancer of zeste homolog-2/vasohibin 1 pathway via vascular endothelial growth factor secretion, thereby promoting the proliferation and angiogenesis of human umbilical vein endothelial cells. **Conclusion:** Our study identified the relationship between cancer-associated fibroblasts and enhancer of zeste homolog-2 and confirmed the pivotal role of cancer-associated fibroblasts in angiogenesis of hepatocellular carcinoma. Cancer-associated fibroblasts promote angiogenesis of hepatocellular carcinoma by vascular endothelial growth factor-mediated enhancer of zeste homolog-2/vasohibin 1 pathway and may be a potentially useful therapeutic target for hepatocellular carcinoma.

Keywords

CAFs, angiogenesis, EZH2, hepatocellular carcinoma, VASH1

Abbreviations

α -SMA, α -smooth-muscle actin; CAFs, cancer-associated fibroblasts; CM, conditioned medium; CM-CAFs, condition medium of CAFs; CM-NFs, condition medium of NFs; DAPI, 4,6-diamidino-2-phenylindole; ECs, endothelial cells; ELISA, enzyme-linked immunosorbent assay; EZH2, enhancer of zeste homolog 2; FAP, fibroblast activation protein; FBS, fetal bovine serum; HCC, hepatocellular carcinoma; HUVECs, human umbilical vein endothelial cells; mRNA, messenger RNA; MTT,

¹ Department of Intervention, Hunan Provincial Cancer Hospital, Changsha, People's Republic of China

² Department of Gynecology, Affiliated Hospital of Hunan Institute of Traditional Chinese Medicine, Changsha, People's Republic of China

Corresponding Author:

Qin Li, Department of Gynecology, Affiliated Hospital of Hunan Institute of Traditional Chinese Medicine, Changsha 410009, People's Republic of China.
Email: liqinlq2017123112@163.com



3-(4,5-Dimethylthiazol-2-yl)-2,5-diphenyltetrazolium bromide; NFs, noncancerous fibroblasts; OD, optical density; PBS, phosphate-buffered saline; qRT-PCR, quantitative real-time polymerase chain reaction; RPMI, Roswell Park Memorial Institute; SD, standard deviation; shRNA, short hairpin RNA; VASH1, vasohibin 1; VEGF, vascular endothelial growth factor.

Received: January 02, 2018; Revised: February 24, 2019; Accepted: August 13, 2019.

Introduction

Hepatocellular carcinoma (HCC) is the fifth most common cancer worldwide¹ with a very high degree of malignancy² and an extremely poor prognosis.³ Nowadays, the effective treatments of HCC include surgery, radiotherapy, chemotherapy, biological therapy, and so on. Despite the use of innovative therapeutic strategies for HCC, survival rate is still poor for patients with HCC.² Tumor angiogenesis and metastatic spreading are 2 highly interconnected phenomena, contributing to cancer-associated deaths.⁴ The establishment of new blood vessels, derived from preexisting ones, provides growing tumors with nutrients and oxygen⁵; therefore, the induction of angiogenesis is considered to be one of the hallmarks of cancer.⁶ In addition, angiogenesis plays a vital role in tumor progression and metastasis.⁷ Meanwhile, HCC is a highly vascularized tumor,⁸ so it is critical to study its angiogenesis.

It is worth noting that the local microenvironment is thought to be an active participant in the process of tumor initiation, progression, and metastasis.⁹ Meanwhile, tumor cells properly interact with their surrounding host microenvironment for tumor progression.¹⁰ Recent studies gradually focused on cancer-associated fibroblasts (CAFs), and the prominent role of CAFs in promoting tumor growth and progression¹¹ has been the subject of extensive research in the fields of tumor. Earlier studies indicated that CAFs promoted tumor growth by inducing angiogenesis¹¹ and invasion.¹² These results have been identified and especially true for HCC.¹³

Enhancer of zeste homolog 2 (EZH2), a catalytic component of the polycomb repressor complex 2,¹⁴ has intrinsic histone methyl transferase activity,¹⁴ thereby silencing multiple tumor suppressor genes.⁴ Upregulation of EZH2 promotes cell growth, migration, and invasion. High level of EZH2 expression is associated with poor prognosis, high grade, and high stage.⁴ Nowadays, a new study has proved that EZH2 plays an important role in tumor angiogenesis¹⁵ and has been implicated in the progression and metastasis of certain cancers.¹⁶ These findings were further confirmed by Lu *et al*'s report, which showed that the role of EZH2 in tumor angiogenesis has also been discovered in nasopharyngeal carcinoma.⁴ In addition, endothelial gene expression and function was also regulated by EZH2,^{14,17} such as mediated regulation of vasohibin 1 (VASH1), which is an endothelial cell-specific and intrinsic negative regulator of angiogenesis.¹⁸ However, although the abundant evidence revealed that tumor microenvironment, especially CAFs and EZH2, can mediate the angiogenesis, the relationship between EZH2 and CAFs in response to angiogenesis has not been reported.

In this study, we started from investigating the potential involvement of CAFs in tumor proliferation and angiogenesis. Thus, we focused on evaluating the mechanism of CAFs in promoting angiogenesis in human umbilical vein endothelial cells (HUVECs). Our study will provide useful targets to develop novel and more effective antiangiogenic therapy.

Materials and Methods

Reagents

Antibodies specific for α -smooth muscle actin (α -SMA; ab5694), fibroblast activation protein (FAP, ab53066), EZH2 (ab186006), VASH1 (ab199732), CD31 (ab28364), Alexa Fluor 647-conjugated second antibody (ab150087), and β -actin (ab8229) and recombinant protein vascular endothelial growth factor (VEGF; ab168684) were purchased from Abcam (Cambridge, United Kingdom). Goat anti-rabbit fluorescein isothiocyanate-conjugated secondary antibodies (AP307F) were obtained from Sigma-Aldrich Inc (St Louis, Missouri). The EZH2 inhibitor GSK126 (HY-13470) was purchased from MedChem Express (Monmouth Junction, New Jersey, USA). The VEGF was used at 300 nM and GSK126 at 9.9 nM. The cell proliferation reagent methylthiazolyldiphenyl-tetrazolium bromide (MTT) was purchased from Roche (Mannheim, Germany). Human VEGF enzyme-linked immunosorbent assay (ELISA) kit was purchased from Multi-Sciences (Hangzhou, China).

Cell Culture

Both HUVECs and HepG2 cells were purchased from the China Infrastructure of Cell Line Resources (Beijing, China) and American Type Culture Collection (Manassas, Virginia), respectively. The HUVECs were cultured in 60-mm plates in endothelial basal medium containing 1% fetal bovine serum (FBS) and endothelial cell growth medium 2 Bullet Kit in a humidified atmosphere of 5% CO₂ at 37°C. And HepG2 cells were cultured in Roswell Park Memorial Institute 1640 (RPMI 1640) medium supplemented with 10% FBS, 1% penicillin/streptomycin, and 2% L-glutamine at 37°C in a humidified atmosphere of 5% CO₂.

Isolation of Primary Fibroblasts From HCC Specimens

Tumor samples were obtained from patients with HCC (Hunan Provincial Cancer Hospital, Changsha, China). Samples were anonymously coded in accordance with local ethical guidelines (as stipulated by the Declaration of Helsinki), and written

informed consent was obtained from patients and healthy volunteers. The work was conducted in strict accordance with the study design as approved by the Clinical Research Ethics Committee of the Hunan Provincial Cancer Hospital.

Cancer-associated fibroblasts were isolated from the cancerous region and noncancerous fibroblasts (NFs) taken from paracancer. The tissues were minced and digested in RPMI 1640 (Invitrogen, Carlsbad, California) supplemented with 10% FBS (Gibco-BRL, Grand Island, New York), 1 mg/mL collagenase type I (Sigma, St Louis, Missouri) and 100 U/mL hyaluronidase (Sigma-Aldrich Inc, St Louis, Missouri) at 37°C for 6 to 8 hours, washed twice with phosphate-buffered saline (PBS; Sigma-Aldrich Inc), and centrifuged at 450g for 8 minutes each time. They were finally resuspended in RPMI 1640 supplemented with 10% FBS, 100 IU/mL penicillin, 100 µg/mL streptomycin, and then cultured at 37°C in a humidified 5% CO₂ environment. The percentage of purified fibroblasts was about 100% after 2 to 3 passages, which was determined by immunofluorescence using antibody against α-SMA and FAP. Subsequent experiments were carried out using these cells within 3 to 10 passages.¹⁹

To prepare the conditioned medium (CM), CAFs and NFs were cultured for 72 hours and the CM was collected and centrifuged for 10 minutes at 3000 rpm to remove cell debris. All *in vitro* experiments were performed in triplicate using 2 pairs of CAFs and NFs which were less than 10 passages.²⁰

Immunofluorescence

Cells were cultured in a 24-well plate and washed twice with PBS. The cells were then fixed with 4% paraformaldehyde, permeabilized with 0.2% Triton X-100, and blocked with 1% bovine serum albumin (Beyotime, Shanghai, China) in PBS for 30 minutes. The cells were incubated with a primary antibody α-SMA (1:200) and FAP (1:150). Fluorescein isothiocyanate-conjugated (green) and Alexa Fluor 647-conjugated (red) goat anti-rabbit were used as secondary antibody. The nuclei were counterstained using 4,6-diamidino-2-phenylindole (Biotium, Fremont, California). Images were obtained with an FV1000 laser scanning confocal microscope (Olympus, Nagoya, Japan).

RNA Interference and Transfection

Short hairpin RNA (shRNA) sequences for VEGF and VASH1 were designed and synthesized from Shanghai Gene Pharma Co Ltd (Shanghai, China). The resulting oligonucleotides sequences were termed sh-VEGF and sh-VASH1. Short hairpin RNA with a scrambled nonspecific sequence was used as a negative control (sh-NC). The sequences of the used shRNA oligonucleotides were: sh-VEGF, sense: 5'-GATCCGCCTCCGAAACCATGAACTTTTCAAGAGAAAGTTCATGGTTTCGGAGTTTTTTACGCGTG-3', antisense: 5'-AATTCACGCGTAAAAACCTCCGAAACCATGAACTTTCTCTTGAAAGTTCATGGTTTCGGAGGCG-3'; sh-VASH1, sense: 5'-CAACGCAATCAAATGCCTGGAAGCCGAAGCTTCCAGG

CATTTGATTGGC-3', antisense: 5'-AAAAGCCAATCAAATGCCTGGAAGCTTCGGCTTCCAGGCATTTGATTGGC-3'. When the CAFs or HUVECs were grown to 60% confluence, sh-VEGF and sh-NC plasmids or sh-VASH1 and sh-NC plasmids were, respectively, transfected into cells using Lipofectamine 2000 reagent (Invitrogen, Thermo Fisher Scientific, Inc, Waltham, Massachusetts, USA) according to the manufacturer's protocol. Then the medium was changed 6 to 10 hours after transfection to avoid the problem of toxicity. Following 48-hour transfection, the cells were collected for use in subsequent experiments.

Methylthiazolyldiphenyl-Tetrazolium Bromide Assay

The effect of CAFs on cell viability was assessed by MTT assay as described previously.²¹ Briefly, 5 × 10³ HUVECs were seeded in 96-well plate and cultured for 12 hours; condition medium of CAFs (CM-CAFs), VEGF, GSK126, the CM-CAFs, CM-CAFs + sh-VEGF or the VEGF/GSK126 combination, and saline were added to the cells. After additional 24, 48, or 72 hours of respective treatments, 20 µL of MTT (5 mg/mL) was added into the wells and cells were incubated for 4 hours. Media were removed and replaced with 100 µL dimethyl sulfoxide. Plates were read on a plate reader (BioRad Laboratories, Hercules, California) at 490 nm, and the reference wavelength was 690 nm. Inhibition of cell growth was measured as the percentage of viable cells relative to the control and calculated as follows: percentage of viable cells rate = 100% × OD_T/OD_C, where OD_T is the average optical density (OD) value of the treated samples and OD_C is the average OD value of the control samples. The assay was repeated 3 times. The mean OD ± standard deviation (SD) was calculated for each group.

In Vitro Wound Healing Assay

Cells were seeded in 6-well plates until confluent. A mechanical wound was created by gently scratching the cells with the tip of a pipette (time 0 hour).²² The cells were then washed with serum-free medium and cultured in RPMI 1640 medium with 0.1% FBS. Images were captured after 48 hours, and the relative migration distance was calculated using the following formula: the relative migration distance (%) = 100 (AX - BX)/(A blank - B blank), where A is the width of the cell wound before incubation and B is the width of the cell wound after incubation.²³ Experiments were carried out in triplicate wells from 3 independent experiments.

Transwell Invasion Assay

The assay was performed using chambers containing polycarbonate filters (8-µm pore size; Merck Millipore, Darmstadt, Germany). The upper side of a polycarbonate filter was coated with Matrigel (BD Biosciences, Franklin Lakes, New Jersey) to form a continuous, thin layer. Human umbilical vein endothelial cells (1 × 10⁵) were resuspended in 300 µL of 0.1% serum medium and then added to the upper chamber. The lower chamber was filled with CM from CAFs or NFs (200 µL). After a 24-hour incubation

and removal of the cells from the upper chamber of the filter with a cotton swab, the cells on the underside were stained with 1% crystal violet and then counted under microscope.

Vascular Tube Formation Assay In Vitro

Plates with 24 wells were first coated with Matrigel (BD Biosciences). Unpolymerized Matrigel was placed in the wells (300 μ L/well) and allowed to polymerize for 1 hour at room temperature. Human umbilical vein endothelial cells in 500 μ L medium were seeded onto the polymerized Matrigel at a density of 5×10^4 cells/well.²⁴ After stimulated overnight, images of tube formation were acquired with an inverted phase-contrast light microscope (Olympus Corporation, Tokyo, Japan). The degree of tube formation was quantified in 5 random fields from each well at 40 \times magnification, using ImageJ software (version 1.48, National Institutes of Health, Bethesda, Maryland).²²

Enzyme-Linked Immunosorbent Assay

To measure the expression level of VEGF, supernatant was collected from the CM-CAFs and condition medium of NFs (CM-NFs) cells when cultured for 48 hours. Supernatant was collected and applied to ELISA kit (Multi-Sciences, Hangzhou, China), according to the manufacturer's instructions.

Quantitative Real-Time Polymerase Chain Reaction Analysis

Quantitative real-time polymerase chain reaction (qRT-PCR) analysis was performed as described previously.²³ Glyceraldehyde 3-phosphate dehydrogenase (GAPDH) messenger RNA (mRNA) was used to normalize the RNA inputs. The sequences of the upstream and downstream primers were, respectively, as follows: sense: 5'-AGG ACGGCTCCTCTAACCAT-3', antisense: 5'-AGCGGC TCCACAAGTAAGAC-3' for EZH2 (245 bp); sense: 5'-GAGCCAGAAGAGGAAGGGGA-3', antisense: 5'-GGTATGGGGATCTTGGGCAG-3' for VASH1 (191 bp); sense: 5'-GTCCACTGGCGTCTTCACC-3', antisense: 5'-ATGAGTCCTTCCACGATACCAA-3' for GAPDH (234 bp).

Western Blotting

Cells were harvested and lysed with RIPA lysis buffer (Beyotime Biotechnology, Shanghai, China). The total proteins were quantified by Bradford protein assay kit (PIERCE, Waltham, Massachusetts, USA). The proteins were separated by sodium dodecyl sulfate polyacrylamide gel electrophoresis and transferred into polyvinylidene difluoride membrane. Membranes were blocked in blocking buffer (5% nonfat dry milk/0.1% Tween 20 in Tris-buffered saline) for 1 hour at room temperature, before being incubated at 4°C with the appropriate antibody in blocking buffer. The membranes were washed and incubated with the appropriated peroxidase-conjugated secondary antibody. After washing, the protein level was detected using electrochemiluminescence (ECL) reagents (GE Healthcare, USA).²⁵

β -actin was chosen as an internal control, and the blots were probed with mouse β -actin mAb. Anti-rabbit (Pierce, 1:6000 dilution) or anti-mouse HRP-conjugated antibodies (Pierce, 1:3000 dilution) were used for secondary antibody reactions.

Animal Model of Tumor Xenografts

Athymic nude mice (female, 5-6 weeks old) were purchased from Beijing Vital River Laboratory Animal Technology Co, Ltd. Animals were housed (5 per cage) in specific pathogen-free condition, supplied with food and water ad libitum, and kept on a 12-hour light-dark cycle. All studies were conducted in accordance with the Institutional Animal Care and Use Committee approved protocols. HepG2 cells (5×10^6), CAFs (5×10^6) combined with HepG2 cells (5×10^6), or sh-VEGF-CAFs (5×10^6) combined with HepG2 cells (5×10^6) were suspended in PBS and subcutaneously planted in the right dorsal flank of the mice. All the mice were observed and examined daily for the formation of nodules at the site of injection. After 4 weeks, mice were euthanized and the tumors removed and photographed. Tumor weight was measured.

Immunohistochemistry Staining

Immunohistochemistry staining was performed using Biotin-Streptavidin HRP Detection Kit (Zhongshan Bio, Beijing, China), according to the manufacturer's procedure.²⁵ In brief, tumor tissues obtained from HepG2, CAFs combined with HepG2, or sh-VEGF-CAFs combined with HepG2 nude mice xenografts were formalin fixed, paraffin embedded, and then cut into 5- μ m sections. After antigen retrieval with autoclaving in citric acid, and inactivating endogenous peroxidase with 3% H₂O₂, the slides were incubated with the rabbit anti-mouse CD31 monoclonal antibody (1:100 dilution; Abcam) overnight at 4°C. Second antibody conjugated with biotin was applied for 1 hour at room temperature. Then the sections were developed in 3,3-diaminobenzidine and counterstained with hematoxylin.

Statistics

All experiments were performed in triplicate, and the results were expressed as the mean \pm SD. Statistical significance was determined using the GraphPad Prism V5.0 software (GraphPad Software, La Jolla, California). Student *t* test was used to analyze statistical differences between the 2 groups. Differences between multigroups were studied using analysis of variance followed by post hoc tests (Dunnett, Tukey). Differences were considered statistically significant at *P* < .05. Error bars indicate \pm SD.

Results

Cancer-Associated Fibroblasts Promote Angiogenesis of HUVECs

Cancer-associated fibroblasts were isolated from primary tumor tissues and cultured according to the methods described

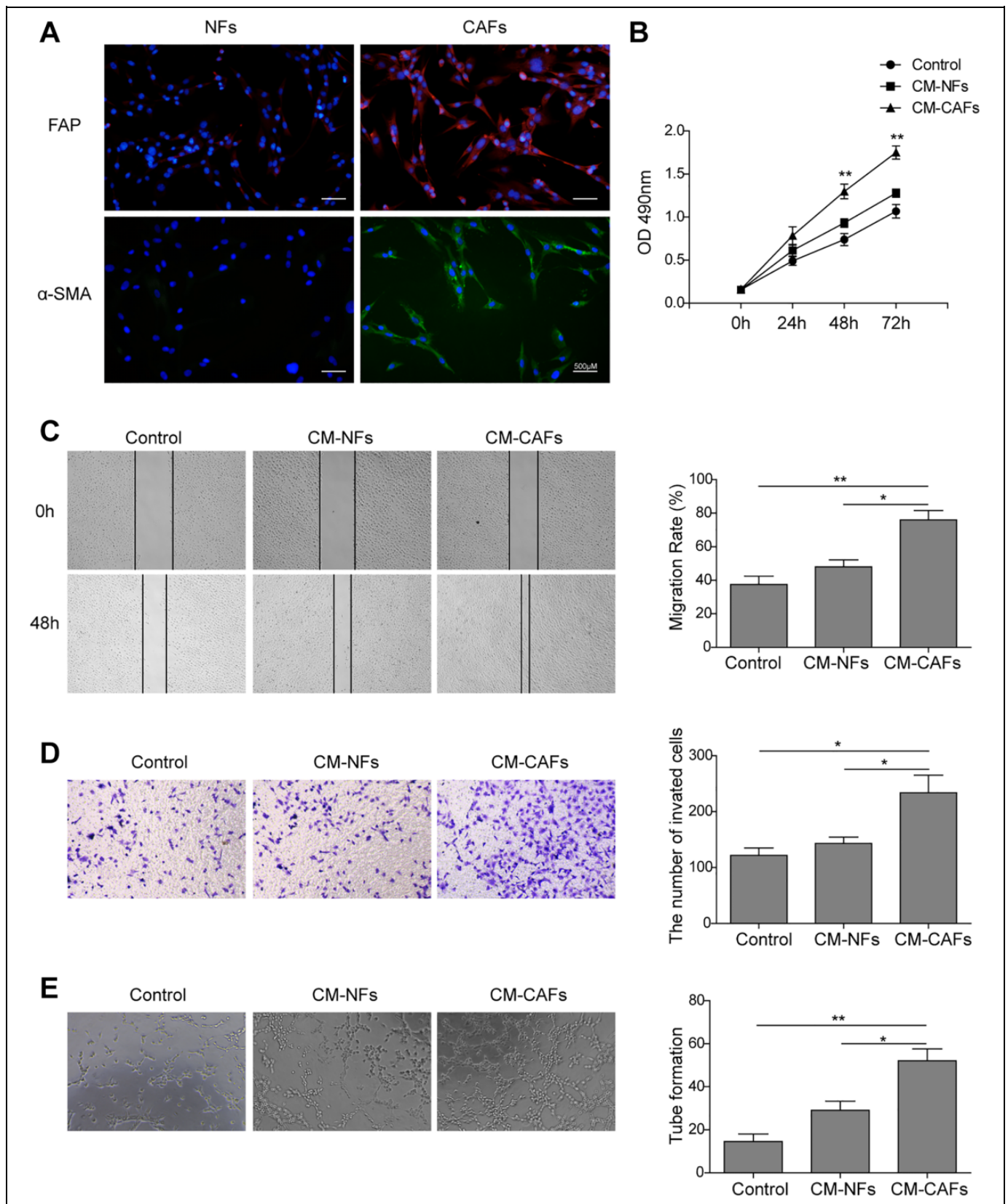


Figure 1. Cancer-associated fibroblasts promote angiogenesis in HUVECs. A, Cancer-associated fibroblasts were isolated from primary liver tumor tissues. The cells (5×10^3) were grown in 24-well plate for 24 hours, fixed, permeabilized, and stained with primary antibody (α -SMA or FAP). Fluorescein isothiocyanate-conjugated (green) and Alexa Fluor647-conjugated (red) goat anti-rabbit were used as secondary antibody.

in previous study.¹⁹ Previously, studies have shown that CAFs can be identified by their expression of vimentin, desmin, α -SMA, and FAP.¹² Here, we found CAFs show a high-level expression of α -SMA and FAP according to the immunofluorescence analysis (Figure 1A), which shows the percentage of purified fibroblasts was about 90% after 2 to 3 passages.

To further identify the effect of CAFs on angiogenesis in HUVECs, the CM harvested from the culture supernatant of NFs (CM-NFs) and CAFs (CM-CAFs) was used to culture HUVECs, respectively. The effect on the proliferation of HUVECs was examined by MTT assay. As presented in Figure 1B, HUVEC proliferation at 24 hours exhibited no significant difference between the groups, while at 48 hours, cell proliferation in the CM-CAFs group was slightly higher than that in the control and CM-NFs groups ($P < .01$). The CM-CAFs also significantly promoted the proliferation of HUVECs compared to that of the control and CM-NFs groups at 72 hours ($P < .01$).

Furthermore, to determine the effect of CM-CAFs on the migration and invasion of HUVECs, wound healing and transwell assays were performed. As shown in Figure 1C (left), the wound healing capacity of HUVECs was enhanced obviously by CM-CAFs at 48 hours after the wounds were created. According to the quantitative comparison of cell migration distances at 48 hours (Figure 1C, right), the migration rate in the CM-CAFs group was significantly higher than that in the control group ($P < .01$), suggesting that the migration of HUVECs was enhanced by CM-CAFs. However, the migration rate in the CM-NFs group was not significantly different from that in the control group ($P > .05$), which suggested that, different from CM-CAFs, CM-NFs may not affect the migration of HUVECs. Similarly, CM-CAFs significantly induced the invasion of HUVECs (Figure 1D).

Moreover, it was examined whether CM-CAFs were able to promote endothelial network formation through Matrigel assay. Human umbilical vein endothelial cells were plated onto Matrigel; then cells were cultured with CM-CAFs or CM-NFs overnight. The microphotographs were then obtained (Figure 1E, left), and the number of tube-like structure branch points was quantitatively analyzed (Figure 1E, right). As presented in Figure 1D (right), a significant increase in the tube formation in the CM-CAFs group was observed ($P < .01$), where normal tube structures were formed. The CM-NFs groups also promoted the number of tube formations, but the tube structures observed in this group were as irregular as those in the control groups.

Cancer-Associated Fibroblasts Promote Angiogenesis of HUVECs via VEGF Secretion In Vitro

To examine the angiogenesis effects of CAFs, we compared the expression level of VEGF in the CM-CAFs and CM-NFs. The ELISA results showed that a significantly higher level of VEGF was detected in the CM-CAFs group (Figure 2A), indicating that there was a significantly increase in VEGF secretion in the CM-CAFs group compared to that in the CM-NFs group ($P < .01$).

Next, we tested whether CAFs promoted the proliferation and angiogenesis of HUVECs through VEGF; the influence of CM-CAFs on tube formation of HUVECs was detected *in vitro*. First, the vectors that expressed shRNA against VEGF or sh-NC were transfected into CAF cells, which showed sh-VEGF significantly reduced the endogenous VEGF level in CAF cells (Figure 2B). And then the culture supernatant of sh-VEGF CAF cells (CM-CAFs + sh-VEGF) was harvested and used to incubate HUVECs. Then, the effect on the proliferation of HUVECs was examined by MTT assay. As shown in Figure 2C, the proliferation of HUVECs was significantly increased in both CM-CAFs and VEGF groups, but the treatment with CM-CAFs + sh-VEGF group obviously abrogated the CM-CAFs-enhanced proliferation. Furthermore, wound healing assay showed that the cell migration was significantly increased in the CM-CAFs and VEGF groups, while this phenomenon was reversed in the CM-CAFs + sh-VEGF group (Figure 2D; $P < .01$). Besides, the Transwell assay also showed that the cell invasion was enhanced in the CM-CAFs and VEGF groups; however, the CM-CAFs + sh-VEGF blocked the CM-CAFs-enhanced invasion (Figure 2E; $P < .01$). In addition, tube formation results also indicated that the capability of tube formation was remarkably enhanced when the HUVECs were incubated with CM-CAFs or VEGF as angiogenic stimuli; however, the treatment with CM-CAFs + sh-VEGF also evidently abrogated the enhanced tube formation (Figure 2F; $P < .01$), suggesting that CAFs contributed to the angiogenesis via VEGF. Taken together, these results indicate that CAFs promote angiogenesis of HUVECs via VEGF secretion.

Cancer-Associated Fibroblasts Promote Angiogenesis via VEGF Secretion In Vivo

To further verify the CAFs promote angiogenesis via VEGF secretion *in vivo*, HepG2 cells (5×10^6), sh-VEGF-CAFs and HepG2 combination ($5 \times 10^6 + 5 \times 10^6$), or CAFs and HepG2 combination ($5 \times 10^6 + 5 \times 10^6$) were, respectively, injected

Figure 1. (Continued). Noncancerous fibroblasts were used as control. Nuclei were counterstained with DAPI (blue staining). Scale bar represents 500 μ m. B, Analysis of cell growth rate by modified MTT assay. C, Conditioned medium CAFs enhanced the wound healing capacity of HUVECs at 48 hours after scratching (left). Quantification of cell migration distances at 48 hours after scratching (right). D, The invasion of HUVECs treated with control, CM-NFs, and CM-CAFs were determined by Transwell assays (magnification, $\times 100$). E, Human umbilical vein endothelial cells plated onto Matrigel to form tube-like structures in the 3 groups were observed under an inverted phase-contrast microscope (left). Scale bars, 100 μ m. Quantification of tube-like structure branch points (right). Each experiment was repeated for at least 3 times. Error bars indicate \pm SD. * $P < .05$, and ** $P < .01$. α -SMA, α -smooth-muscle actin; CAFs, cancer-associated fibroblasts; CM, conditioned medium; DAPI, 4,6-diamidino-2-phenylindole; FAP, fibroblast activation protein; HUVEC, human umbilical vein endothelial cell; MTT, 3-(4,5-dimethylthiazol-2-yl)-2,5-diphenyltetrazolium bromide; NFs, noncancerous fibroblasts; SD, standard deviation.

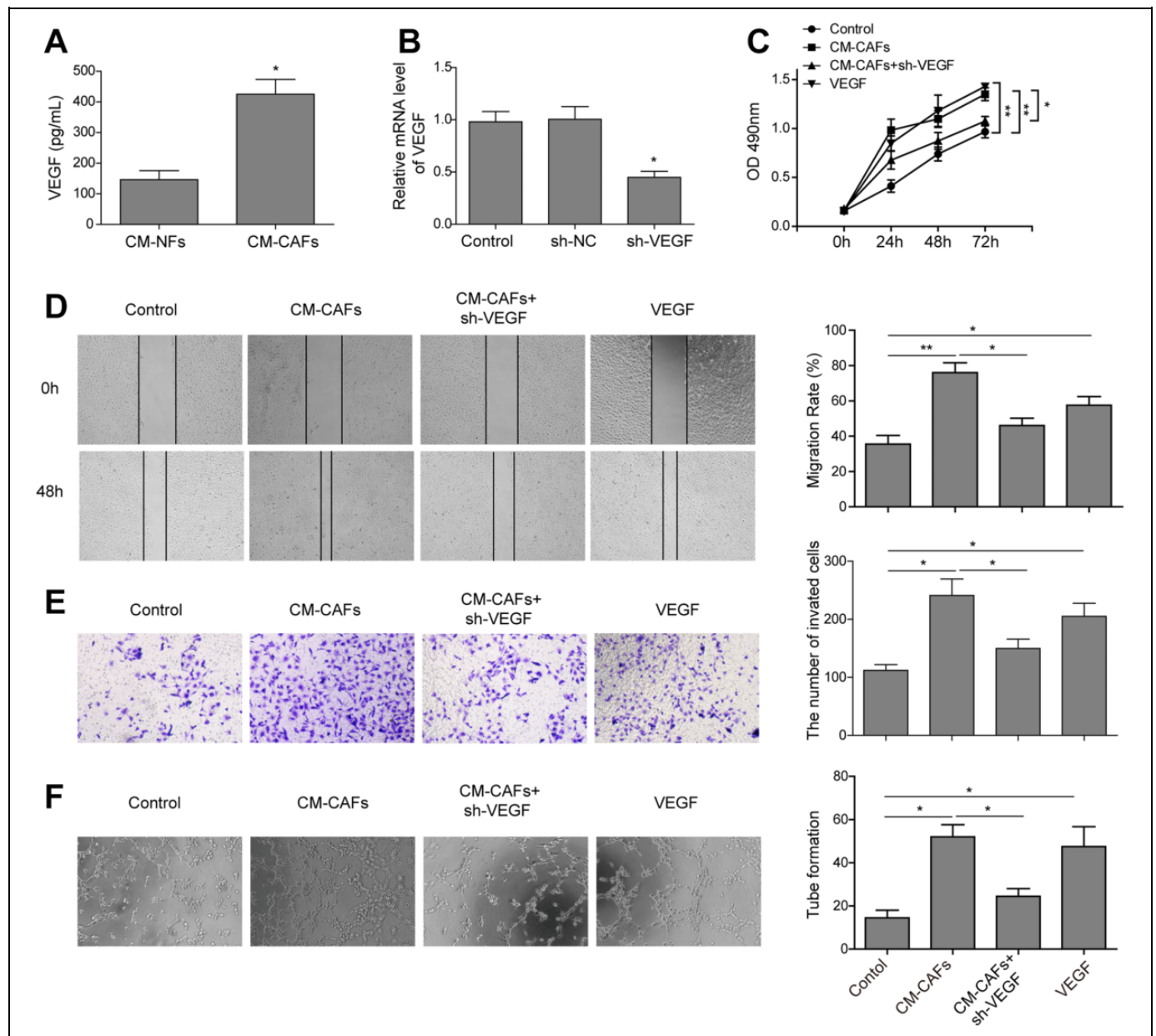


Figure 2. Cancer-associated fibroblasts promote angiogenesis of HUVECs via VEGF secretion *in vitro*. A, Enzyme-linked immunosorbent assay analysis for VEGF showed that the amount of VEGF significantly increased in the CM-CAFs. B, Vascular endothelial growth factor was detected using qRT-PCR after the transfection of CAFs with sh-VEGF. C, 3-(4,5-Dimethylthiazol-2-yl)-2,5-diphenyltetrazolium bromide assay was used to analyze the proliferation of HUVECs. The proliferation of HUVECs was significantly inhibited in the CM-CAFs and Vascular endothelial growth factor receptor inhibitor combination group compared to the CM-CAFs and VEGF groups. D, Representative images for wound healing assay (left) and quantification of cell migration distances after scratching (right). E, The invasion of HUVECs treated with CM-CAFs, VEGF, or CM-CAFs + sh-VEGF was determined by Transwell assays (magnification, $\times 100$). F, Images of tube-like structures in the 3 groups (left) and quantification of tube-like structure branch points (right) were shown. Conditioned medium CAFs promoted the tube formation of HUVECs, and VEGFR inhibitor reversed the CAFs-induced promotion effect. Error bars indicate the SD from at least triplicate determinations. * $P < .05$, ** $P < .01$, and *** $P < .001$. CAFs indicates cancer-associated fibroblasts; CM, conditioned medium; ELISA, enzyme-linked immunosorbent assay; HUVEC, human umbilical vein endothelial cell; qRT-PCR, Quantitative real-time polymerase chain reaction; SD, standard deviation; VEGF, vascular endothelial growth factor; VEGFR, vascular endothelial growth factor receptor.

into nude mice. As shown in Figure 3A and B, the tumors of the CAFs and HepG2 combination group grew dramatically compared to the HepG2 group; however, the tumor size and weight between HepG2 group and sh-VEGF-CAFs and HepG2 combination group were almost equal. In addition, we assayed for

the endothelial cell marker CD31 using immunohistochemistry (Figure 3C). The result showed that CAFs significantly increased the expression of CD31, while knockdown VEGF in CAF cells significantly reversed the promotion on the expression of CD31 induced by CAFs, indicating sh-VEGF

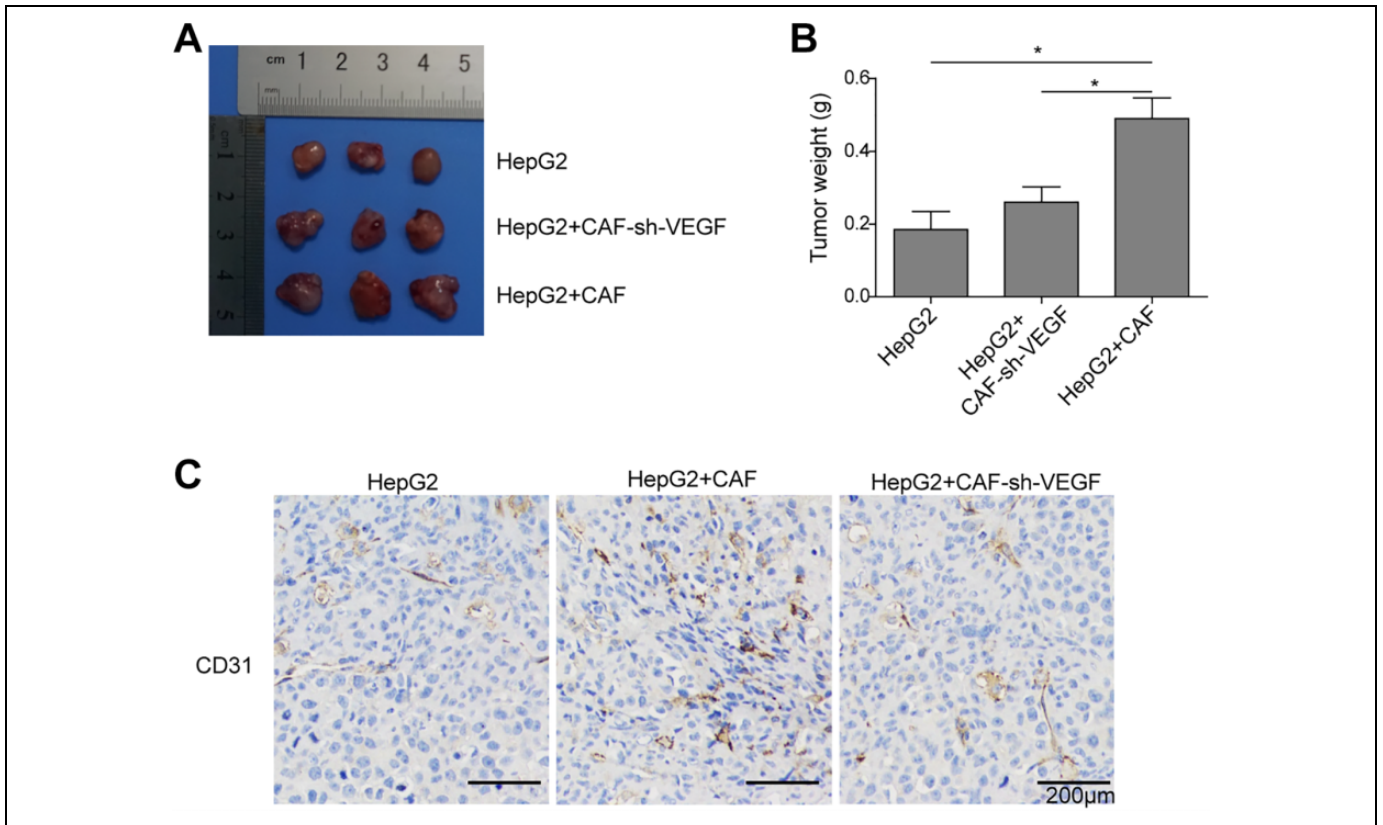


Figure 3. Cancer-associated fibroblasts promote angiogenesis via VEGF secretion *in vivo*. HepG2 cells (5×10^6), sh-VEGF-CAFs and HepG2 combination ($5 \times 10^6 + 5 \times 10^6$), or CAFs and HepG2 combination ($5 \times 10^6 + 5 \times 10^6$) were, respectively, injected into nude mice. After 4 weeks, all mice were euthanized and autopsied. A, Photograph of tumors obtained from the different groups of nude mice. B, Tumor weight was calculated. C, Representative images of immunohistochemical staining for CD31 in tumor tissues. Scale bar in CD31 represents 200 µm. Error bars indicate the standard deviations (SD) from at least triplicate determinations. * $P < .05$, ** $P < .01$. CAFs indicates cancer-associated fibroblasts; VEGF, vascular endothelial growth factor.

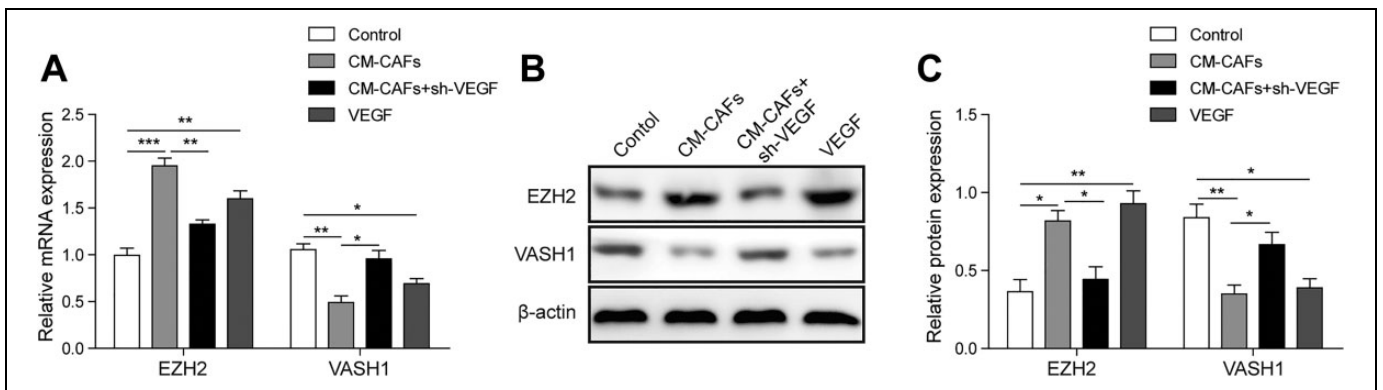


Figure 4. Vascular endothelial growth factor upregulates EZH2 expression of HUVECs. A, Relative qRT-PCR analysis of EZH2 and VASH1. GAPDH serve as reference control. B, Enhancer of zeste homolog 2 and VASH1 were detected using Western blotting after treatment of HUVECs with CM-CAFs, VEGF, or CM-CAFs + sh-VEGF. β-actin was used as reference control. All data were represented as the mean \pm SD from at least triplicate experiments. * $P < .05$, ** $P < .01$, and *** $P < .001$. CAFs indicates cancer-associated fibroblasts; CM, conditioned medium; EZH2, enhancer of zeste homolog 2; HUVEC, human umbilical vein endothelial cell; qRT-PCR, Quantitative real-time polymerase chain reaction; SD, standard deviation; VASH1, vasohibin 1; VEGF, vascular endothelial growth factor.

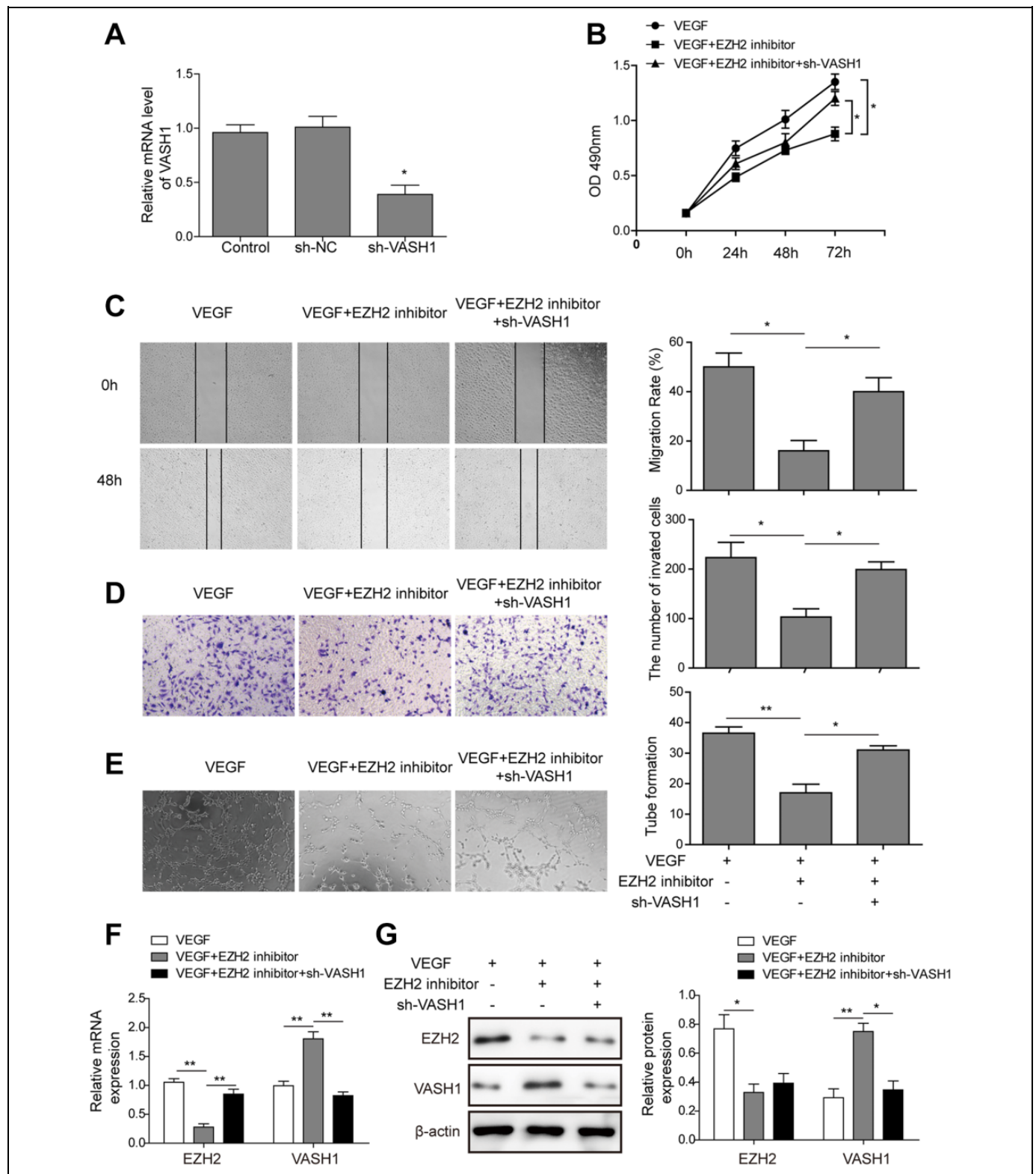


Figure 5. Enhancer of zeste homolog inhibits the proliferation and angiogenesis of HUVECs by upregulation of VASH1. A, The expression level of VASH1 was detected by qRT-PCR after the transfection of HUVECs with sh-VASH1. B, The MTT assay was used to analyze cell growth rate after treatment of HUVECs with VEGF, VEGF + EZH2 inhibitor (GSK126), or VEGF + EZH2 inhibitor + sh-VASH1. C, The wound healing capacity of HUVECs in VEGF, VEGF + EZH2 inhibitor (GSK126), or VEGF + EZH2 inhibitor + sh-VASH1 groups at 48 hours after scratching (left). Quantification of cell migration distances at 48 hours after scratching (right). D, The invasion of sh-VASH1-HUVECs treated with VEGF combined with GSK126 was determined by Transwell assays (magnification, $\times 100$). E, Representative examples

suppressed CAFs-induced tumor angiogenesis, that is, CAFs could promote angiogenesis of HUVECs via VEGF secretion *in vivo*.

Vascular Endothelial Growth Factor Upregulates EZH2 Expression in HUVECs

Research had found that VEGF increased EZH2 levels in endothelial cells and EZH2-mediated regulation of VASH1.¹⁴ To determine the mechanism that CAFs regulating the proliferation and angiogenesis of HUVECs via VEGF, we further investigated the expression level of EZH2 and VASH1 by qRT-PCR and Western blot. Compared to the control group, the expression level of EZH2 was obviously upregulated in the CM-CAF and VEGF groups compared to the control group (Figure 4A and B; $P < .01$). However, the level of EZH2 was downregulated in the CM-CAFs + sh-VEGF group compared to the CM-CAFs and VEGF groups (Figure 4A and B, $P < .01$).

Since EZH2 levels were noted to be upregulated in the CM-CAFs and VEGF groups, we next asked whether the expression level of VASH1, downstream molecular of EZH2, was downregulated. Results of qRT-PCR and Western blot indicated that the expression level of VASH1 was downregulated in the CM-CAF and VEGF groups compared to the control group (Figure 4A and B; $P < .01$), while the level of VASH1 was upregulated in the CM-CAFs + sh-VEGF group compared to the CM-CAFs and VEGF groups (Figure 4A and B, $P < .01$). These results indicated that VEGF may inhibit the expression of VASH1 by upregulating the expression of EZH2, thereby promoting the proliferation and angiogenesis of HUVECs.

Inhibition of EZH2 Inhibits the Proliferation and Angiogenesis of HUVECs by Upregulation of VASH1

To further identify the function of EZH2, VEGF was used as angiogenic stimuli for HUVECs. Initially, sh-VASH1 and sh-NC plasmids were, respectively, transfected into HUVECs. As shown in Figure 5A, the expression level of VASH1 was significantly downregulated ($P < .05$) in the sh-VASH1-HUVECs compared to sh-NC-HUVECs. Then, after adding GSK126 (EZH2 inhibitor), cell proliferation, migration, invasion, and tube formation were observed. The MTT assay indicated that the proliferation of HUVECs was significantly inhibited in the VEGF and GSK126 combination group (VEGF + EZH2 inhibitor) compared to the VEGF group (Figure 5B; $P < .05$); however, knockdown of VASH1 significantly reduced the inhibition on cell proliferation induced by EZH2 inhibitor ($P < .05$, when compared to VEGF + EZH2 inhibitor cells). Next, we performed a wound healing and Transwell assay. As shown in

Figure 5C and D, the invasion and migration ability of HUVECs were abolished by GSK126 ($P < .05$), and sh-VASH1 significantly rescued the inhibitor effect of GSK126. Furthermore, Matrigel assay results showed that there was a significant decrease in the tube formation in the VEGF and GSK126 combination group. Meanwhile, knockdown of VASH1 promoted the angiogenesis of HUVECs compared to GSK126 group under VEGF condition (Figure 5E).

In addition, the mRNA and protein levels of EZH2 remarkably decreased; however, striking increase in VASH1 expression was observed in the VEGF and GSK126 combination group (Figure 5F and G); however, sh-VASH1 unaffected the expression of EZH2 but decreased the expression of VASH1 when treated with VEGF combined with GSK126 (Figure 5F and G). Therefore, the knockdown of VASH1 in HUVECs could reverse the inhibition of GSK126 on the proliferation, migration, invasion, and angiogenesis, which revealed VEGF promotes cell proliferation and angiogenesis of HUVECs via EZH2/VASH1 pathway.

Discussion

Previous research have recognized and highlighted the importance of the local tumor microenvironment to tumor progression¹¹ and the role during carcinogenesis.¹⁹ Carcinoma-associated fibroblasts are one of the most crucial components of the HCC microenvironment.²⁶ It has been reported that tumor angiogenesis is a highly interconnected phenomena, contributing to cancer-associated deaths,⁴ and is regulated by the balance of various proangiogenic stimulators, such as VEGF, and other angiogenesis inhibitors.¹⁴ Thus, understanding the mechanisms that CAFs promote angiogenesis of HCC is extremely crucial.

In this work, we first successfully isolated specific CAFs from primary HCC tissues. Then, we reported that CAFs could promote proliferation and angiogenesis of HUVECs. Recently, multiple studies have reported that CAFs are activated in a wound healing process²⁷ and promote tumor proliferation, invasion, and metastasis via secretion of various growth factors and degradation of extracellular matrix proteins.²⁸ Consistent with these studies, we found that the migration and invasion capacity of HUVECs is enhanced obviously by CM-CAFs. Moreover, a significant increase in the tube formation in the CM-CAFs groups is also observed. Accumulating evidence indicates that angiogenesis is regulated by the balance of various proangiogenic stimulators, such as VEGF.¹⁴ Jia *et al* reported that CAFs stimulate malignant cell proliferation by providing different types of growth factors.¹⁹ The results from our present study show that there was a significantly higher

Figure 5. (Continued). of tube formation were shown (left). Quantification of tube-like structure branch points (right). F and G, The expression level of EZH2 and VASH1 at the mRNA (F) and protein (G) levels. The bars represent each sample performed in triplicate, and the error bars represent mean \pm SD. * $P < .05$, ** $P < .01$, and *** $P < .001$. CAFs indicates cancer-associated fibroblasts; CM, conditioned medium; EZH2, enhancer of zeste homolog-2; HUVEC, human umbilical vein endothelial cell; mRNA, messenger RNA; MTT, 3-(4,5-dimethylthiazol-2-yl)-2,5-diphenyltetrazolium bromide; qRT-PCR, quantitative real-time polymerase chain reaction; SD, standard deviation; VASH1, vasohibin 1; VEGF, vascular endothelial growth factor.

level of VEGF in the CM-CAFs. In addition, sh-VEGF reversed CM-CAFs-induced proliferation, invasion, migration, and tube formation of HUVECs *in vitro*. We also demonstrated that CAFs could promote the tumor growth and angiogenesis; however, sh-VEGF-inhibited CAFs induced tumor growth and angiogenesis *in vivo*. These data suggested that CAFs promote proliferation and angiogenesis of HUVECs via VEGF secretion.

Existing studies have shown that EZH2 is a key regulator of cancer angiogenesis in ovarian and other cancers²⁹ and could impact specific angiogenic mechanisms of cancer angiogenesis.⁴ Vasohibin 1 is also known to inhibit endothelial cell migration, proliferation, and tube formation.¹⁴ Furthermore, VASH1 expression can be induced by VEGF as part of a negative feedback mechanism in endothelial cells.³⁰ Besides, the increase in endothelial EZH2 is a direct result of VEGF stimulation by a paracrine circuit that promotes angiogenesis by methylating and silencing VASH1, and EZH2 silencing increases VASH1 in endothelial cells.¹⁴ Here, we showed that the expression level of EZH2 was obviously upregulated, while the expression level of VASH1 was downregulated in the CM-CAFs and VEGF groups. However, the downregulation of VASH1 was reversed by adding CM-CAFs + sh-VEGF. We also found that the inhibition of EZH2 could inhibit the proliferation and angiogenesis of HUVECs by upregulation of VASH1. In short, VEGF inhibited the expression of VASH1 by upregulating the expression of EZH2, thereby promoting the proliferation and angiogenesis of HUVECs.

In summary, our study identifies that the CAFs of HCC regulate the EZH2/VASH1 pathway via VEGF secretion, thereby promoting the proliferation and angiogenesis of HUVECs. These discoveries further support the impact of CAFs on HCC proliferation and angiogenesis *in vitro* and *in vivo*, with VEGF as an important mediator and then expound the relationship between CAFs and EZH2. This interaction may be an interesting tumor angiogenesis-independent target for therapy. In conclusion, to the extent that targeting CAFs can provide therapeutic benefits might represent novel targets and promising strategies for treatment of HCC.

Declaration of Conflicting Interests

The author(s) declared no potential conflicts of interest with respect to the research, authorship, and/or publication of this article.

Funding

The author(s) received no financial support for the research, authorship, and/or publication of this article.

ORCID iD

Qin Li  <https://orcid.org/0000-0002-9327-550X>

References

- Li T, Yang Y, Hua X, et al. Hepatocellular carcinoma-associated fibroblasts trigger NK cell dysfunction via PGE2 and IDO. *Cancer Lett.* 2012;318(2):154-161.
- Wang H, Huo X, Yang XR, et al. STAT3-mediated upregulation of lncRNA HOXD-AS1 as a ceRNA facilitates liver cancer metastasis by regulating SOX4. *Mol Cancer.* 2017;16(1):136.
- Kuang DM, Zhao Q, Peng C, et al. Activated monocytes in peritumoral stroma of hepatocellular carcinoma foster immune privilege and disease progression through PD-L1. *J Exp Med.* 2009;206(6):1327-1337.
- Lu J, Zhao FP, Peng Z, et al. EZH2 promotes angiogenesis through inhibition of miR-1_Endothelin-1 axis in nasopharyngeal carcinoma. *Oncotarget.* 2014;5(22):11319-11332.
- Julia H, Sandra ME, Pfitze L, et al. Cyclin-dependent kinase 5 stabilizes hypoxia-inducible factor-1 α _ a novel approach for inhibiting angiogenesis in hepatocellular carcinoma. *Oncotarget.* 2016;7(19):27108-27121.
- Bergers G, Hanahan D. Modes of resistance to anti-angiogenic therapy. *Nat Rev Cancer.* 2008;8(8):592-603.
- Azam F, Mehta S, Harris AL. Mechanisms of resistance to anti-angiogenesis therapy. *Eur J Cancer.* 2010;46(8):1323-13232.
- Murakami K, Kasajima A, Kawagishi N, et al. The prognostic significance of vasohibin 1-associated angiogenesis in patients with hepatocellular carcinoma. *Hum Pathol.* 2014;45(3):589-597.
- Hwang RF, Moore T, Arumugam T, et al. Cancer-associated stromal fibroblasts promote pancreatic tumor progression. *Cancer Res.* 2008;68(3):918-926.
- Gong Y, Scott E, Lu R, Xu Y, Oh WK, Yu Q. TIMP-1 promotes accumulation of cancer associated fibroblasts and cancer progression. *PLoS One.* 2013;8(10):e77366.
- Yang T, Chen M, Yang X, et al. Down-regulation of KLF5 in cancer-associated fibroblasts inhibit gastric cancer cells progression by CCL5/CCR5 axis. *Cancer Biol Ther.* 2017;8(10):806-815.
- Liao D, Luo Y, Markowitz D, Xiang R, Reisfeld RA. Cancer associated fibroblasts promote tumor growth and metastasis by modulating the tumor immune microenvironment in a 4T1 murine breast cancer model. *PLoS One.* 2009;4(11):e7965.
- Mazzocca A, Dituri F, Lupo L, Quaranta M, Antonaci S, Giannelli G. Tumor-secreted lysophosphatidic acid accelerates hepatocellular carcinoma progression by promoting differentiation of peritumoral fibroblasts in myofibroblasts. *Hepatology.* 2011;54(3):920-930.
- Lu C, Han HD, Mangala LS, et al. Regulation of tumor angiogenesis by EZH2. *Cancer Cell.* 2010;18(2):185-197.
- Crea F, Fornaro L, Bocci G, et al. EZH2 inhibition: targeting the crossroad of tumor invasion and angiogenesis. *Cancer Metastasis Rev.* 2012;31(3-4):753-761.
- Miura H, Miyazaki T, Kuroda M, et al. Increased expression of vascular endothelial growth factor in human hepatocellular carcinoma. *J Hepatol.* 1997;27(5):854-861.
- Maleszewska M, Vanchin B, Harmsen MC, Krenning G. The decrease in histone methyltransferase EZH2 in response to fluid shear stress alters endothelial gene expression and promotes quiescence. *Angiogenesis.* 2016;19(1):9-24.
- Watanabe K, Hasegawa Y, Yamashita H, et al. Vasohibin as an endothelium-derived negative feedback regulator of angiogenesis. *J Clin Invest.* 2004;114(7):898-907.

19. Jia CC, Wang TT, Liu W, et al. Cancer-associated fibroblasts from hepatocellular carcinoma promote malignant cell proliferation by HGF secretion. *PLoS One*. 2013;8(5):e63243.
20. Wang L, Cao L, Wang H, et al. Cancer-associated fibroblasts enhance metastatic potential of lung cancer cells through IL-6_ STAT3 signaling pathway.pdf. *Oncotarget*. 2017;8(44): 76116-76128.
21. Aras B, Yerlikaya A. Bortezomib and etoposide combinations exert synergistic effects on the human prostate cancer cell line PC-3. *Oncol Lett*. 2016;11(5):3179-3184.
22. Yang MH, Chang KJ, Zheng JC, et al. Anti-angiogenic effect of arsenic trioxide in lung cancer via inhibition of endothelial cell migration, proliferation and tube formation. *Oncol Lett*. 2017; 14(3):3103-3109.
23. Wang SJ, Cui HY, Liu YM, et al. CD147 promotes Src-dependent activation of Rac1 signaling through STAT3_DOCK8 during the motility of hepatocellular carcinoma cells. *Oncotarget*. 2014;6(1): 243-257.
24. Fang X, Hong Y, Dai L, et al. CRH promotes human colon cancer cell proliferation via IL-6/JAK2/STAT3 signaling pathway and VEGF-induced tumor angiogenesis. *Mol Carcinog*. 2017;56(11): 2434-2445.
25. Feng F, Wang B, Sun X, et al. Metuzumab enhanced chemosensitivity and apoptosis in non-small cell lung carcinoma. *Cancer Biol Ther*. 2017;18(1):51-62.
26. Kubo N, Araki K, Kuwano H, Shirabe K. Cancer-associated fibroblasts in hepatocellular carcinoma. *World J Gastroenterol*. 2016; 22(30):6841-6850.
27. Tomasek JJ, Gabbiani G, Hinz B, Chaponnier C, Brown RA. Myofibroblasts and mechano-regulation of connective tissue remodelling. *Nat Rev Mol Cell Biol*. 2002;3(5):349-363.
28. Yamamura Y, Asai N, Enomoto A, et al. Akt-Girdin signaling in cancer-associated fibroblasts contributes to tumor progression. *Cancer Res*. 2015;75(5):813-823.
29. He M, Zhang W, Bakken T, et al. Cancer angiogenesis induced by Kaposi sarcoma-associated herpesvirus is mediated by EZH2. *Cancer Res*. 2012;72(14):3582-3592.
30. Chang CJ, Yang JY, Xia W, et al. EZH2 promotes expansion of breast tumor initiating cells through activation of RAF1-beta-catenin signaling. *Cancer Cell*. 2011;19(1):86-100.